

# Etoposide Treatment of Cancer Cell Lines Results in Nuclear Localisation of Cleaved Gasdermin D

Soukaina Imlilss<sup>1</sup> , Zahira Ahmadi<sup>1</sup> , Ghita Jekki<sup>1</sup> , Elif Eren<sup>1</sup> 

<sup>1</sup>Bahcesehir University, Faculty of Engineering and Natural Sciences Department of Molecular Biology and Genetics, Inflammasomes and Cell Death Laboratory, Besiktas, Istanbul, Türkiye

## ABSTRACT

**Objective:** Overcoming resistance to apoptosis is one of the main goals of cancer treatment. Subversion of apoptosis to pyroptosis, an inflammatory cell death mediated by Gasdermin family members, was previously proposed as an alternative strategy for killing cancer cells. Since the pyroptotic activity of Gasdermin D has been mainly studied in the context of inflammasome activation and its association with cancer is mostly based on expression correlation, we sought to determine whether Gasdermin D-mediated pyroptosis could be triggered in response to drugs used to induce apoptosis in cancer cells.

**Materials and Methods:** Cancer cells were treated with different concentrations of etoposide, gemcitabine, and cisplatin, which are used as chemotherapeutic agents in various ongoing clinical trials. Membrane integrity was evaluated by measuring lactate dehydrogenase release, and Gasdermin D and Caspase activations and subcellular localisation of Gasdermin D were determined by western blotting.

**Results:** Upon treatment with the well-known apoptosis inducer etoposide, a necrotic form of programmed cell death was observed in different cancer cell lines even at low drug concentrations. Additionally, cleavage analysis revealed a 20-kDa-Gasdermin D fragment in the supernatant of treated cells. Surprisingly, this cleaved form was localised in the nuclei of etoposide-treated cells rather than in the well-defined cytosolic and plasma membrane localisations.

**Conclusion:** Overall, these results demonstrate the complex interplay between different cell death pathways and suggest that Gasdermin D generates a fragment presenting an unknown function in the nuclei of etoposide-treated cancer cell lines.

**Keywords:** Pyroptosis, Gasdermin D, Cancer, Etoposide, Nucleus

## INTRODUCTION

Pyroptosis is an inflammatory form of necrotic cell death mediated by Gasdermin D and is required for the clearance of pathogen-infected cells and to trigger inflammation.<sup>1–3</sup> Gasdermin D is activated upon the recognition of pathogen-associated molecular patterns (PAMPs) and danger-associated molecular patterns (DAMPs) by the canonical and non-canonical inflammasome pathways. Gasdermin D cleavage by Caspase-1/4/5 results in the release of the 30 kDa N-terminal fragment (p30), which translocates to the plasma membrane to form pores and induces pyroptosis.<sup>1,2</sup> These pores serve as conduits for IL-1beta secretion into the extracellular milieu and result in membrane rupture through the activation of NINJ1.<sup>4,5</sup>

Before the identification of their role in pyroptosis, the expression of Gasdermin proteins was initially proposed as a prognostic marker for various cancers. For instance, Gasdermin B was shown to be highly expressed in breast cancer, and

new strategies to target Gasdermin B in HER2-positive breast cancer cells are under development.<sup>6,7</sup> Whereas a clear correlation between Gasdermin B expression and cancer progression was made, conflicting results were obtained for Gasdermin D. Although a decrease in Gasdermin D expression was found to activate anti-tumoral immunity, other studies demonstrated that *Gasdermin D* downregulation promoted gastric tumour formation and colorectal cancer.<sup>8–11</sup> These data suggest that Gasdermin proteins modulate cancer through properties beyond their expression.

Interestingly, Gasdermin E, another member of the family, can also trigger pyroptosis under physiological conditions. Gasdermin E was not activated by inflammasome-related Caspases but rather by the apoptotic executioner Caspase-3 and initiator Caspase-8. Gasdermin E triggered secondary necrosis upon its cleavage by Caspase-3 in macrophages infected with vesicular stomatitis virus or treated with high concentrations of etopo-

Corresponding Author: Elif Eren E-mail: elif.eren@bau.edu.tr

Submitted: 02.08.2024 • Revision Requested: 27.09.2024 • Last Revision Received: 12.10.2024 • Accepted: 01.11.2024



This article is licensed under a Creative Commons Attribution-NonCommercial 4.0 International License (CC BY-NC 4.0)

side and localised at the mitochondrial membrane to induce the release of mitochondrial proteins.<sup>12,13</sup> Chemotherapeutic agents including etoposide activated Gasdermin E-dependent pyroptosis in different cancer cell lines.<sup>14</sup> Similarly, agents such as lobaplatin, cisplatin, and paclitaxel triggered Gasdermin E-mediated pyroptosis or secondary necrosis in lung and colon cancer cell lines.<sup>15,16</sup> Based on these findings, Gasdermin E is considered the main player at the crossroads of the apoptosis and pyroptosis forming a molecular determinant of pyroptosis induction and is proposed to be a key target to overcome the apoptosis resistance of cancer cells.<sup>14,16-22</sup>

These exciting advances establishing that Caspases involved in apoptosis can also regulate Gasdermin E-dependent pyroptosis/secondary necrosis, led to the discovery of new Gasdermin D cleavage sites. Whereas the activation of Gasdermin D in macrophages stimulated pyroptosis, when *Gasdermin D* was knocked out, Caspase-3 and Caspase-8 activations in response to inflammatory stimuli directed cells towards apoptosis.<sup>23</sup> Gasdermin D-mediated pyroptosis was blocked by Caspase-3 cleavage of Gasdermin D at aspartic acid 87 (Asp87) residue to form a p43 fragment in macrophages.<sup>24</sup> Interestingly, inhibition of TAK1 during *Yersinia* infection unmasked a Caspase-8-dependent Gasdermin D cleavage at Asp275 as well as Gasdermin E activation and pyroptosis.<sup>25,26</sup> Under these conditions, Caspase-3 generated the Gasdermin D p43 band which levels decreased in Caspase-3 knockout cells.<sup>26</sup> Taken together, these findings indicate that Caspase-8 activation in the extrinsic pathway of apoptosis results in Gasdermin D cleavage at Asp275 and pyroptosis, whereas this activation is counteracted by Caspase-3 cleavage at Asp87.<sup>27,28</sup>

Despite these groundbreaking findings in immune cells and under gene knockout or inhibitory conditions, the effect of the well-studied inflammasome-related Gasdermin D protein's pyroptotic activity on tumour cell death is less understood. The present study aimed to determine whether Gasdermin D-mediated pyroptosis could be triggered by treatment with drugs that induce apoptosis in cancer cells. For this purpose, we analysed pyroptosis properties such as cellular morphology, lactate dehydrogenase (LDH) release, Gasdermin D and Caspase activation, IL-1beta secretion and revealed the cellular localisation of Gasdermin D in cancer cell lines treated with etoposide, gemcitabine, and cisplatin, which are known apoptosis-inducers used alone or in combination with other drugs, in numerous ongoing clinical trials.

## MATERIALS AND METHODS

### Cells and Drug Treatments

A549 human lung cancer cell line, HeLa human cervical cancer cell line, THP-1 human leukaemia cell line, and 4T1 mouse breast cancer cell line were used in this study. A549 and HeLa cells were maintained in DMEM and THP-1 and 4T1 cells in RPMI, both supplemented with 10% fetal bovine serum, 1 mM

penicillin/streptomycin, and 1 mM non-essential amino acids. Cells were grown at 37°C, and 5% CO<sub>2</sub>.

2 x 10<sup>6</sup> low passage healthy cells were seeded in a 25 cm<sup>2</sup> flask before treatment. The next day, cells were treated with the indicated concentrations of etoposide (Sigma E1383), gemcitabine (Sigma G6423), and cisplatin (Santa Cruz sc200896) for 24 h. Dimethyl sulfoxide (DMSO)-treated cells were used as a control.

### Morphological Analysis

The morphology of cells was assessed for different drugs, and images were taken at 24 h after drug treatment from randomly chosen fields with the approximate same number of total cells using an inverted light microscope (Olympus CKX41). Necrotic and apoptotic cells were identified visually based on morphological criteria, such as apoptotic body formation for apoptosis and swelling, and nucleus visibility for pyroptosis.

### LDH Assay

LDH levels in fresh cell-free supernatants collected 24 h after drug treatments were measured using the CyQUANT™ LDH Cytotoxicity Assay (Invitrogen #C20301) according to the manufacturer's recommendations. Briefly, 50 µL of fresh supernatant was incubated for 30 min with 50 µL substrate mix and assay buffer, and LDH levels were measured at 490 and 680 nm after stopping the reaction with 50 µL sulphuric acid. DMSO-treated cells were used as negative controls for LDH release, and Triton-X-treated cells were used as positive controls. The percentage of cell death was calculated according to the following formula: ((LDH of the sample - LDH of the negative control)/(LDH of positive control - LDH of negative control))\*100. Each condition was performed in three biological replicates, and LDH levels were measured in triplicate for each biological replicate.

### Inhibition of Membrane Rupture

To inhibit NINJ1-dependent membrane rupture, cells were treated with 5 mM glycine.<sup>29</sup> Glycine was added to the cell supernatant at the same time with the different drugs for membrane inhibition, whereas the other cells were only treated with the drugs. All supernatants were collected 24 h after treatment for the LDH assay.

### Gasdermin D and Caspase Activation

Gasdermin D and Caspase-1, Caspase-8 and Caspase-3 activations were assessed by Western blotting in total cell lysates (TCL) and supernatants (Sup.). For TCL, cells were harvested in RIPA buffer containing protease inhibitor complex and cleared via centrifugation. FBS-free supernatants from con-

control and drug-treated cells were prepared by precipitating proteins with 10% trichloroacetic acid and acetone wash. Both TCL and the supernatants were run on 12% acrylamide gel and transferred to 0.2  $\mu\text{m}$  PVDF membrane for 1 h at 100 V. Proteins were visualised by using anti-Gasdermin D (Abcam #ab209845), anti-Caspase-1 (Cell Signaling Technologies #3866), anti-Caspase-8 (Cell Signaling Technologies #9746), and anti-Caspase-3 (Abcam #ab13847) antibodies.

### IL-1beta Quantification

IL-1beta levels were quantified in the cell-free supernatants of treated cells using a human IL-1beta ELISA kit (Thermo Fischer Scientific, Invitrogen #88-7261). Briefly, plates were coated with anti-IL-1beta capture antibody overnight at 4°C. The next day, after saturation, cell supernatants were added in triplicate, and after 2 h of incubation, biotin-conjugated anti-IL-1beta detection antibodies were added for 2 h. After several washes and 15 min of incubation with tetramethylbenzidine, IL-1beta levels were measured at 450 nm after stopping the reaction. Purified human IL-1beta standards were used to determine the IL-1beta concentration of the samples. Interferon gamma-primed cells infected with logarithmic phase *Salmonella typhimurium* MOI25 for 5 h were used as positive control for IL-1beta secretion.

### Cell Fractionation

After 24 h of treatment, cells were collected and dissociated in 200  $\mu\text{L}$  of hypotonic buffer (20 mM Tris-pH 7.4, 10 mM NaCl, 3 mM  $\text{MgCl}_2$ ). After 15 min of incubation on ice, 12.5  $\mu\text{L}$  of Triton-X100 (10%) was added, and samples were centrifuged for 10 min at 3000 rpm. The supernatant was transferred into a new tube and used as the “cytoplasmic fraction”. The cell pellet was resuspended in 50  $\mu\text{L}$  of complete cellular fractionation buffer (20 mM Tris-pH 7.4, 1% Triton X-100, 10 mM NaCl, 1 mM EDTA, 10% glycerol, 0.1 M SDS) and incubated for 30 min on ice. After 30 min of centrifugation at 14,000 rpm, the supernatant was transferred into a new tube and labeled as the “nuclear fraction”. Equal concentration of total proteins for both nuclear and cytosolic fractions was run on gel, and the purity of each fraction was determined using anti-Lamin A/C antibody (GeneTex #GTX101126) and anti-GAPDH antibody (GeneTex #GTX100118), respectively.

### Statistical Analysis

Statistical analysis was performed using GraphPad Prism version 10.2.3. The two-tailed Student's t-test was used to determine statistical significance. Results of the analysis are shown on graphics with the following symbols: ns: non-significant, \* $p < 0.05$ , \*\* $p < 0.01$ , \*\*\* $p < 0.001$ , \*\*\*\* $p < 0.0001$ . Each experi-

ment was repeated at least three times. Representative images of each experiment were shown.

## RESULTS

### Lytic Form of Cell Death Is Induced in Etoposide-Treated Cell Lines

Etoposide, a known inducer of apoptosis<sup>30</sup>, was also found to trigger NINJ1-dependent plasma membrane rupture and Gasdermin D and Gasdermin E cleavage-associated pyroptosis and/or secondary necrosis in macrophages in previous publications.<sup>26</sup> To test whether it could trigger Gasdermin D-dependent pyroptosis in cancer cells, we treated A549 human lung cancer cell lines with different concentrations of etoposide and determine whether cells could undergo a lytic form of cell death (Figure 1). Twenty-four hours after treatment, etoposide-treated cells started to show morphological characteristics of necrosis, including cell swelling, membrane rupture, and appearance of the nucleus, even at very low concentrations, whereas the DMSO-treated control cells remained intact. These phenotypes were also observed in cells treated with gemcitabine, but at a lower extent than etoposide, whereas cisplatin treatment did not induce significant morphological differences (Figure 1A).

Because the major difference between apoptosis and necrosis is the rupture of the membrane in the latter, we measured the amount of LDH, a high-molecular-weight molecule that can exit the cell only when the membrane is ruptured.<sup>31</sup> Etoposide treatment of A549 cells triggered the release of LDH in approximately 6%, 11%, and 26% of cells at 5, 10 and 50  $\mu\text{M}$  respectively (Figure 1B). Similarly, gemcitabine treatment triggered 1%, 11%, and 13% cell death at 1, 10 and 50  $\mu\text{M}$  respectively (Figure 1C). Although cisplatin is a well-defined apoptosis inducer, it has previously been shown that A549 cells are resistant to cisplatin-induced cell death.<sup>32,33</sup> Similarly, we did not detect any cell death at 20  $\mu\text{M}$  concentration in cisplatin-treated cells or LDH release, demonstrating the absence of cell rupture (Figure 1D).

Recent publications have shown that NINJ1 is activated downstream of many necrotic cellular demise and triggers plasma membrane rupture through its insertion into the plasma membrane.<sup>5,34,35</sup> To further validate membrane lysis upon etoposide treatment suggested by LDH release, we pre-treated cells with or without glycine, an inhibitor of membrane rupture.<sup>29</sup> A statistically significant reduction in LDH levels was observed in the presence of glycine, suggesting that etoposide and gemcitabine disrupted membrane integrity (Figure 1E). To validate whether the induction of necrosis by etoposide is not specific to A549 cells, we treated THP-1 human leukaemia cell lines, HeLa human cervical cancer, and mouse 4T1 breast cancer cell lines with different concentrations of etoposide. Although at different extents, all three cell lines trig-

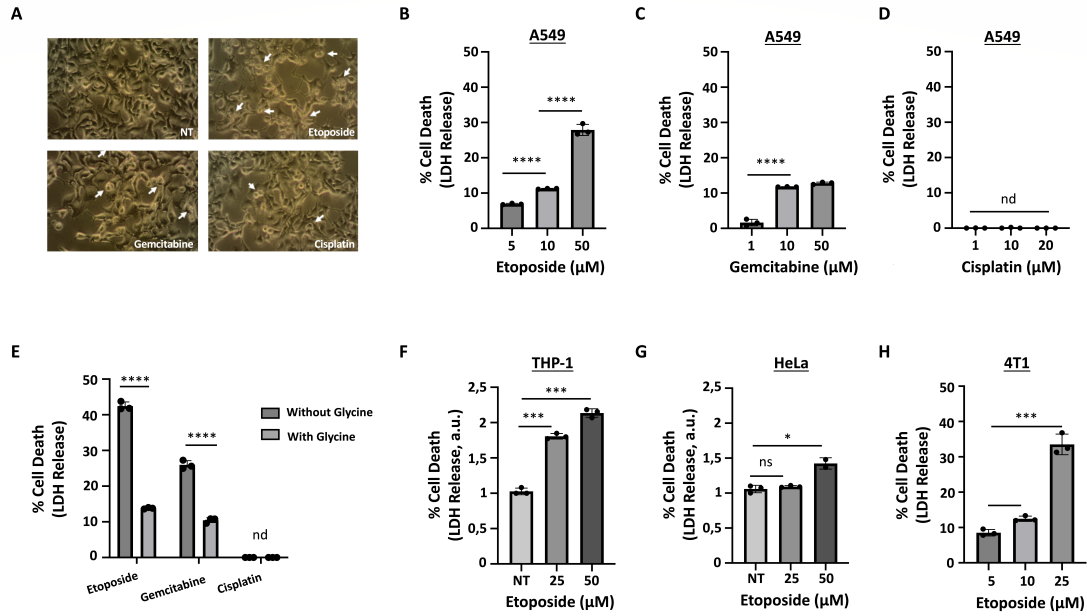


**Figure 1.** Etoposide induces necrotic cell death in cancer cell lines. A. Morphologies of untreated (NT), etoposide (50 μM), gemcitabine (10 μM), and cisplatin (20 μM) treated A549 cells are shown. Arrows indicate pyroptotic cells. B-D. LDH levels were determined in the cell-free supernatant of A549 cells treated with the indicated concentrations of etoposide (B), gemcitabine (C), and cisplatin (D). E. LDH levels in the presence and absence of the plasma rupture inhibitor glycine are given for A549 cells. Nd: not detected. F-H. LDH levels were determined in the cell-free supernatants of etoposide-treated HeLa (F), THP-1 (G), and 4T1 (H) cells. LDH levels were represented in arbitrary units (a.u) for HeLa and THP-1 cells, where the lowest optical density measured for the non-treated (NT) control sample was assigned and 1 arbitrary unit.

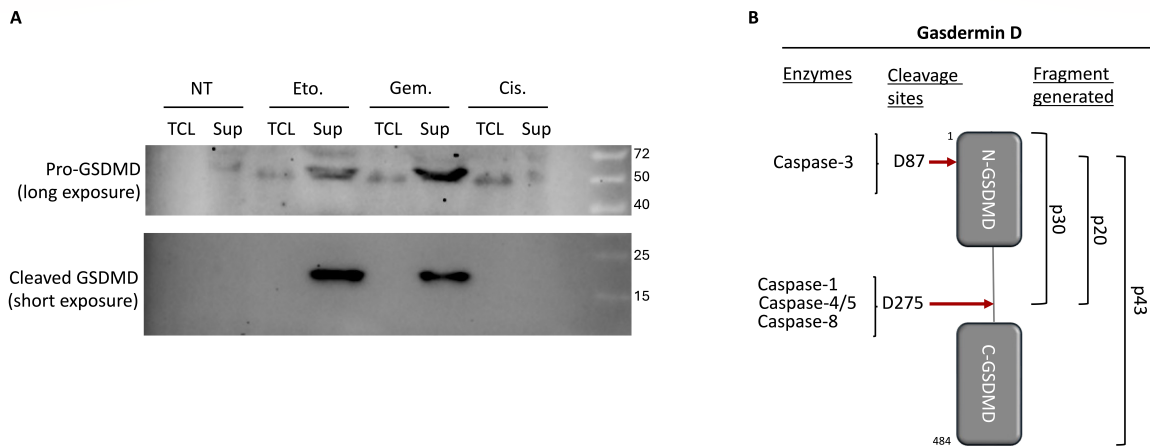


**Figure 2.** Etoposide triggers non-canonical Gasdermin D cleavage. A. Western blot analysis of Gasdermin D cleavage in total cell lysate (TCL) and cell supernatants (Sup). Etoposide and gemcitabine treatments generate a cleaved Gasdermin D band of approximately 20 kDa. A representative image of two sets of experiments is shown. B. Known cleavage sites of human Gasdermin D. Gasdermin D is cleaved at D275 (Asp275) by Caspase-1, Caspase-4/5<sup>1,2</sup>; by Caspase-8 at the same site<sup>25,27</sup>, generating a p30 fragment that triggers pyroptosis. Caspase-3 cleaves human Gasdermin D at D87, resulting in a p43 fragment and p20 fragment.<sup>23,24,27</sup> The protein size was not scaled for the Gasdermin D representation.

gered LDH release, confirming that the phenotype observed in A549 cells is not an experimental artefact (Figure 1F-1H). These data demonstrate that etoposide and gemcitabine induce necrotic cell death resulting in plasma membrane lysis.

### Etoposide Treatment Triggers Gasdermin D Cleavage

Pyroptosis is a form of cell death mediated by Gasdermin proteins.<sup>1,2,36</sup> To determine whether the type of necrotic cell death observed was pyroptosis, we assessed Gasdermin D activation upon apoptotic drug treatment (Figure 2A). In line with our previous results, etoposide and gemcitabine treatments induced Gasdermin D activation by cleavage (Figure 2A). The

active band was secreted outside these cells and was observed only in the supernatants. Gasdermin D has two known Caspase cleavage sites at Asp275 and Asp87 (Figure 2B). Surprisingly, although the antibody that we used recognised the N-terminal of Gasdermin D, we could only detect a cleaved band of approximately 20 kDa (p20) instead of 30 kDa (p30) and/or 43 kDa (p43) (Figure 2A). These results suggest that etoposide treatment triggers Gasdermin D cleavage into an approximately 20-kDa band that could be responsible for pyroptosis induction in A549 lung cancer cells.

### **Etoposide Treatment Activates Different Caspases but Does Not Trigger IL-1beta Secretion**

In order to identify the enzyme responsible for the generation of this 20-kDa form of Gasdermin D, we analysed whether Caspase-3, Caspase-8, and Caspase-1, previously described to cleave Gasdermin D downstream different stimuli, were activated in response to apoptotic drug treatment. Caspase-3 and Caspase-8 were processed by all three drugs into their 25-kDa and 18-kDa active fragments, respectively (Figure 3A). Whereas these fragments were present in the supernatants of etoposide- and gemcitabine-treated cells, they were retained in the cell lysate of cisplatin-treated cells, demonstrating once more the absence of membrane lysis in cisplatin-treated cells (Figure 3A). On the contrary, a 20-kDa cleaved Caspase-1 band could not be detected in either cell lysates or supernatants (Figure 3A).

Besides triggering pyroptosis, the second major role of Gasdermin D is to form pores at the plasma membrane to allow the specific secretion of cleaved IL-1beta outside the cell.<sup>4</sup> Quantification of IL-1beta in the supernatants demonstrated that although present in high concentration in *Salmonella typhimurium-infected* cells used as positive controls, in our experimental settings triggering cleavage of Gasdermin D, IL-1beta secretion was not detected (Figure 3B). In summary, etoposide and gemcitabine treatments activated Caspase-3 and Caspase-8 without inducing Caspase-1 cleavage and IL-1beta secretion.

### **The Cleaved New Gasdermin D Fragment Localises To The Nucleus**

Since Gasdermin D was activated in our model and showed only a 20-kDa band but did not trigger IL-1beta secretion, we hypothesised that this active Gasdermin D fragment might have another cellular function than forming pores at the plasma membrane. To determine the cellular localisation of Gasdermin D upon apoptotic drug treatment, subcellular fractionation was performed (Figure 4). Although the nuclear and cytosolic fractions of etoposide-treated cells were clean, as suggested by Lamin A/C and GAPDH blots, slight cytosolic contamination was present in non-treated cells. Surprisingly, we detected

the cleaved Gasdermin D p20 fragment in the nuclear fraction of etoposide-treated cells (Figure 4). The inactive pro-form or other cleavage forms were absent. These results indicate that the cleavage fragment of Gasdermin D generated by etoposide treatment translocates to the nucleus of cancer cells.

## **DISCUSSION**

To clarify the role of Gasdermin D-induced pyroptosis in cancer cell clearance, we treated cancer cell lines with different concentrations of drugs known to trigger apoptosis and assessed Gasdermin D activation and subcellular localisation. As suspected, the morphological characteristics of pyroptosis, plasma membrane rupture highlighted by LDH release and Gasdermin D cleavage were observed in different cancer cell lines that were used (Figures 1 and 2). To rule out an experimental artefact due to the usage of high concentrations, we lowered the drug concentration down to 10 times their IC<sub>50</sub> and still observed the same phenotype, confirming plasma membrane rupture and Gasdermin D cleavage in these experimental settings (Figure 1). Because prolonged exposure to apoptotic stimuli can trigger secondary necrosis and plasma membrane rupture, the role of Gasdermin E in this process cannot be neglected and must be tested. Nonetheless, these results suggest that etoposide and gemcitabine induce Gasdermin D cleavage followed by plasma membrane rupture. The use of *Gasdermin D*- and *Gasdermin E*-knockout cancer cell lines will determine whether etoposide and gemcitabine trigger pyroptosis or secondary necrosis through Gasdermin D and/or Gasdermin E activation.

Another interesting question that remains to be solved is the identification of the enzyme(s) that cleaved Gasdermin D in response to etoposide and generated the p20 fragment that we observed. According to our results, only Caspase-3 and Caspase-8 were activated in response to etoposide and gemcitabine treatment (Figure 3A). Thus, this band is probably the previously described fragment generated by Caspase-3 and Caspase-8 cleavages at Asp87 and Asp275 residues of full-length or p30 fragment of Gasdermin D.<sup>25-28</sup> Activation of Caspase-3 and Caspase-8 in response to apoptotic stimuli is expected. However, Gasdermin D cleavage is unusual in this context. Gasdermin D-cleaving candidate Caspases should be further confirmed by knocking them out individually or in combination or by using their specific inhibitors. Although plasma membrane rupture triggered by etoposide and gemcitabine was also observed in other cancer cell lines, we could not verify Gasdermin D cleavage in these cells (Figure 1F-1H). Use of other available anti-Gasdermin D antibodies to confirm the presence of the p20 band in other cells would support and validate our data.

Contrary to other publications on macrophages, we did not detect Caspase-1 activation nor IL-1beta cleavage and secretion in the A549 lung cancer cell line (Figure 3). IL-1beta is secreted

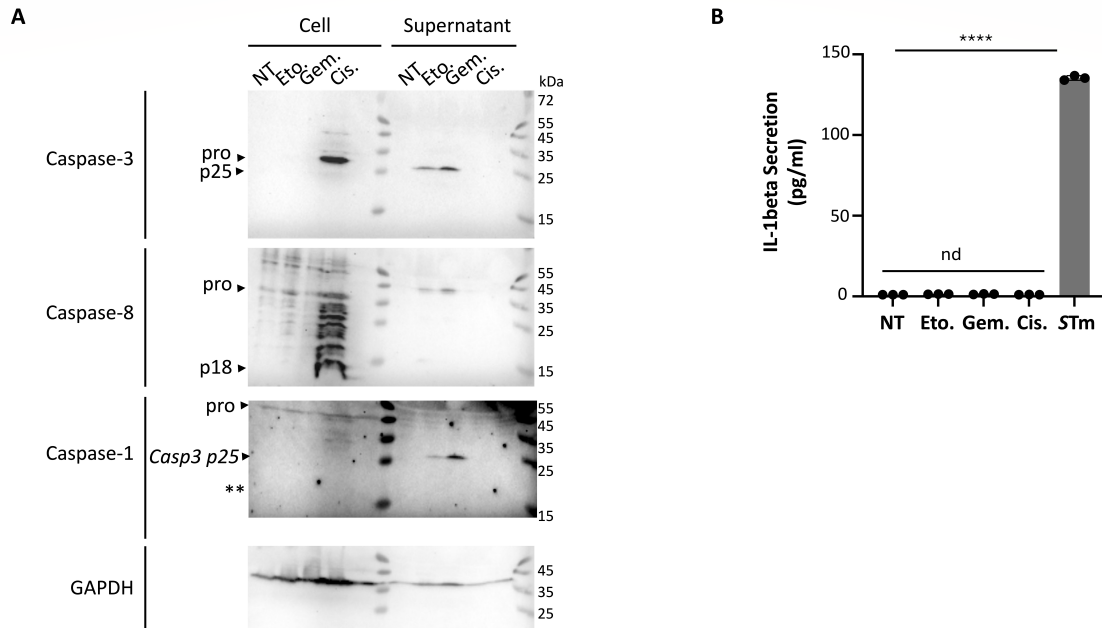


**Figure 3.** Etoposide treatment activates different caspases but does not trigger IL-1beta secretion. **A.** Activation of Caspase-1, Caspase-8 and Caspase-3 was assessed in the cells and supernatants of non-treated (NT), etoposide (50  $\mu$ M), gemcitabine (10  $\mu$ M), and cisplatin (20  $\mu$ M) treated samples. Cleaved forms of Caspase-3 (p25), Caspase-8 (p18) as well as inactive Caspase-3, Caspase-8 and Caspase-1 pro-forms (32 kDa, 42 kDa and 45 kDa respectively) and GAPDH as a loading control are shown. The arrow in the Caspase-1 blot represents cleaved 25-kDa Caspase-3 bands. The expected 20 kDa band of cleaved Caspase-1 was absent. **B.** IL-1beta secretion from the supernatants of cells treated with 50  $\mu$ M etoposide, 10  $\mu$ M gemcitabine and 20  $\mu$ M cisplatin was determined by ELISA. Supernatants of cells infected with *Salmonella typhimurium* SL1344 (STm) for 5 hours were used as positive control for IL-1beta secretion. Nd: not detected. The average of three sets of independent experiments is presented.

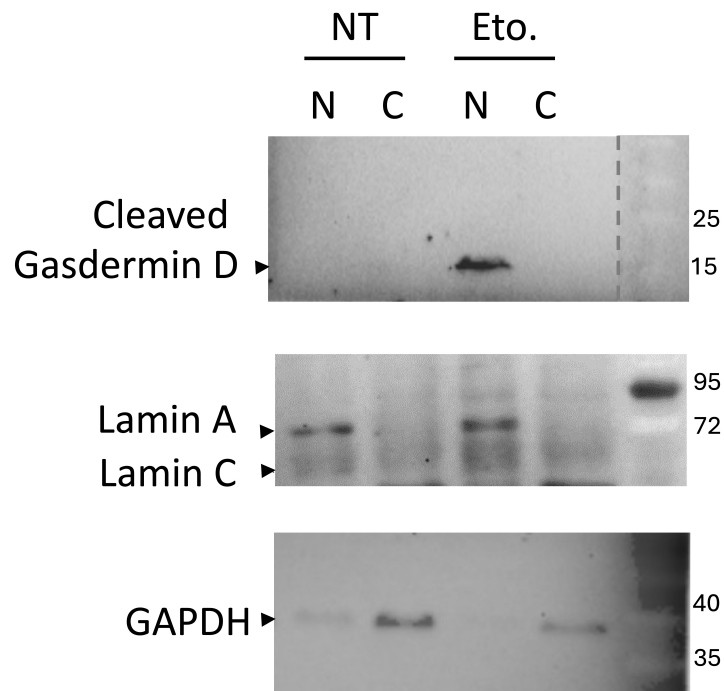


**Figure 4.** Cleaved Gasdermin D fragment localises to the nucleus. Nuclear (N) and cytosolic (C) fractions obtained after subcellular fractionation of non-treated (NT) and etoposide-treated cells are shown. Localisation of cleaved Gasdermin D was determined. Lamin A/C proteins were used as controls for the nuclear fraction, whereas GAPDH was used as control for the cytosolic fraction.

through Gasdermin D pores located at the plasma membrane after maturation by active cleaved Caspase-1.<sup>4,37</sup> The absence of Caspase-1 cleavage justifies the lack of secreted IL-1beta that is probably not cleaved either. Caspase-1 was described to be activated in an inflammasome-dependent manner. In our context, inflammasome complexes are not expected to be activated in response to etoposide treatment. Our data suggest that an inflammasome-independent pyroptosis is triggered and because IL-1beta is not cleaved, it cannot be secreted through Gasdermin pores.

Our findings demonstrated the presence of cleaved Gasdermin D in the supernatant of etoposide-treated cells. To determine whether the detected p20 Gasdermin D band was addressed to the plasma membrane, we performed subcellular fractionation and identified an unexpected nuclear localisation of this fragment (Figure 4). Thus, our data demonstrate an additional role for cleaved Gasdermin D, which was unexpectedly detected in the nucleus of etoposide-treated cancer cells. Gasdermin proteins are usually located in the cytosol of cells in their inactive state and transit to the plasma membrane when activated to form pores.<sup>1,2</sup> Some studies also reported the presence of Gasdermin pores in the mitochondrial membrane leading to mitochondrial membrane rupture and cell death.<sup>13,38</sup> To date, only two publications reported a nuclear localisation of Gasdermin D. Peng et al. demonstrated the translocation of the inactive pro-form of Gasdermin D into the nucleus under the stimulation of chemotherapy drugs in colorectal cancer.<sup>11</sup> In another study, immunohistochemical analysis showed the presence of Gasdermin D in the nucleus, cytoplasm, and plasma membrane of colorectal cancer.<sup>39</sup> Until now, the function of Gasdermin D in the nucleus has been unclear. Contrary to these publications, in our case, not the pro-form but the cleaved form of Gasdermin D was located in the nucleus of etoposide-treated lung cancer cell lines, as observed by subcellular fractionation. Immunostaining of Gasdermin D in treated cells with nuclear markers would confirm our findings.

When the Gasdermin D sequence was analysed, any nuclear localisation or nuclear retention signals could not be detected suggesting that probably a chaperon protein mediates Gasdermin D's transit to the nucleus. Characterisation of the molecular mechanisms of Gasdermin D transport to the nucleus and identification of the role of its pro- and active forms in this cellular compartment would provide significant information on the role of Gasdermin D in cancer. Finally, cancer cell lines maintained in culture were used in our study. We focused on A549 cancer cell lines that showed the highest LDH release, and all our results were based on these cell lines. We validated etoposide-induced plasma membrane rupture in other cell lines, such as THP-1 and HeLa, and both human and mouse cell lines. However, whether Gasdermin D is activated in these cells remains unclear. Determining the exact role of Gasdermin D under normal physiological conditions would provide a better understanding of crosstalk between different pathways. For instance,

tumour samples isolated from patients with cancer could be tested for Gasdermin D cleavage and nuclear localisation. At this point, our results cannot be generalised to all cancer cells. Nonetheless, in the cell line that we were using, we observed a cleaved band with a new subcellular localisation suggesting a novel role for Gasdermin D in cancer that could be masked in other cell lines.

Pyroptotic cells represented not more than 30-40% of the population in our experimental setting, demonstrating that this was not the main mechanism of cell death triggered by etoposide. Morphological analysis also revealed apoptotic cells. Our results do not exclude the induction of secondary necrosis. Even if cleaved Gasdermin D does not trigger pyroptosis or secondary necrosis, it clearly has an undefined role in the nucleus of treated cancer cells. Overall, these data put lights on an uncharacterised mechanism of cleaved Gasdermin D in the nucleus and propose an inflammasome-independent role for Gasdermin D in cancer cells.

## CONCLUSION

The increasing incidence of cancer and the emergence of resistance among tumour cells to apoptosis induced by conventional therapies necessitate the exploration of novel strategies for effectively eradicating these aberrant cells. In this regard, the induction of pyroptosis appears to be a promising approach. In this study, we aimed to characterise the function of Gasdermin D in the interplay between apoptosis and pyroptosis. Similar to other studies, we found that the use of apoptosis inducer drugs triggered plasma membrane rupture in long term (24 h). Gasdermin D was cleaved in response to etoposide and gemcitabine treatments in A549 cancer cell lines, but contrary to other publications, we could only detect the p20 band in the cell supernatants of etoposide- and gemcitabine-treated cells, suggesting double cleavage by Caspase-3 at Asp87 and Caspase-8 at Asp275. Previous studies have investigated the activation of Gasdermin D by apoptotic Caspases in the context of infections and inflammasome activation in macrophages by inhibiting a pathway or knocking out a gene.<sup>23-28</sup> In this study, we demonstrate the cleavage of Gasdermin D into p20 fragment upon etoposide treatment in a cancer cell line. Moreover, we detected a cleaved p20 band in the nucleus of cells. Taken together, our results suggest that the Gasdermin D p20 fragment generated in response to etoposide treatment translocates to the nucleus of cancer cells. Additional experiments are needed to confirm these results, to determine whether the observed cell death is due to Gasdermin D-dependent pyroptosis or Gasdermin E-dependent secondary necrosis/pyroptosis, and to evaluate the physiological relevance of these findings. In conclusion, the present study provides evidence of the connections between different cell death pathways and the interplay between important proteins involved in the apoptosis and pyroptosis in cancer cells. Overall, we propose that Gasdermin D could be a novel

molecular switch between apoptosis and pyroptosis in cancer and unveiled the non-canonical localisation of cleaved p20 Gasdermin D in the nucleus of etoposide-treated cancer cells.

**Ethics Committee Approval:** Ethics committee approval is not required for the study.

**Peer Review:** Externally peer-reviewed.

**Author Contributions:** Conception/Design of Study- E.E., S.I.; Data Acquisition- E.E., S.I., Z.A., G.J.; Data Analysis/Interpretation- E.E., S.I., Z.A., G.J.; Drafting Manuscript- E.E.; Critical Revision of Manuscript- E.E.; Final Approval and Accountability- E.E., S.I., Z.A., G.J.

**Conflict of Interest:** Authors declared no conflict of interest.

**Financial Disclosure:** Authors declared no financial support.

### ORCID IDs of the Authors

Soukaina Imlilss 0009-0001-9488-1931  
 Zahira Ahmadi 0009-0001-9394-9420  
 Ghita Jekki 0009-0004-4892-6803  
 Elif Eren 0000-0002-0328-5609

### REFERENCES

- Kayagaki N, Stowe IB, Lee BL, et al. Caspase-11 cleaves gasdermin D for non-canonical inflammasome signalling. *Nature*. Published online 2015. doi:10.1038/nature15541
- Shi J, Zhao Y, Wang K, et al. Cleavage of GSDMD by inflammatory caspases determines pyroptotic cell death. *Nature*. 2015;526(7575):660-665. doi:10.1038/nature15514
- Jorgensen I, Zhang Y, Krantz BA, Miao EA. Pyroptosis triggers pore-induced intracellular traps (PITs) that capture bacteria and lead to their clearance by efferocytosis. *J Exp Med*. 2016;213(10):2113-2128.
- Heilig R, Dick MS, Sborgi L, Meunier E, Hiller S, Broz P. The Gasdermin-D pore acts as a conduit for IL-1 $\beta$  secretion in mice. *Eur J Immunol*. 2018;48(4):584-592.
- Kayagaki N, Kornfeld OS, Lee BL, et al. NINJ1 mediates plasma membrane rupture during lytic cell death. *Nature*. 2021;591(7848):131-136.
- Hergueta-Redondo M, Sarrío D, Molina-Crespo Á, et al. Gasdermin B expression predicts poor clinical outcome in HER2-positive breast cancer. *Oncotarget*. 2016;7(35):56295-56308.
- Molina-Crespo Á, Cadete A, Sarrío D, et al. Intracellular delivery of an antibody targeting gasdermin-b reduces HER2 breast cancer aggressiveness. *Clin Cancer Res*. 2019;25(15):4846-4858.
- Jiang Y, Yang Y, Hu Y, et al. Gasdermin D restricts anti-tumor immunity during PD-L1 checkpoint blockade. *Cell Rep*. 2022;41(4):111553. doi:10.1016/j.celrep.2022.111553
- Traughber CA, Deshpande GM, Neupane K, et al. Myeloid-cell-specific role of Gasdermin D in promoting lung cancer progression in mice. *iScience*. 2023;26(2):106076. doi:10.1016/j.isci.2023.106076
- Wang WJ, Chen D, Jiang MZ, et al. Downregulation of gasdermin D promotes gastric cancer proliferation by regulating cell cycle-related proteins. *J Dig Dis*. 2018;19(2):74-83.
- Peng X, Na R, Zhou W, et al. Nuclear translocation of Gasdermin D sensitizes colorectal cancer to chemotherapy in a pyroptosis-independent manner. *Oncogene*. 2022;41(47):5092-5106.
- Rogers C, Fernandes-Alnemri T, Mayes L, Alnemri D, Cingolani G, Alnemri ES. Cleavage of DFNA5 by caspase-3 during apoptosis mediates progression to secondary necrotic/pyroptotic cell death. *Nat Commun*. 2017;8:14128. doi:10.1038/ncomms14128
- Rogers C, Erkes DA, Nardone A, Aplin AE, Fernandes-Alnemri T, Alnemri ES. Gasdermin pores permeabilize mitochondria to augment caspase-3 activation during apoptosis and inflammasome activation. *Nat Commun*. 2019;10(1):1689. doi:10.1038/s41467-019-09397-2
- Wang Y, Gao W, Shi X, et al. Chemotherapy drugs induce pyroptosis through caspase-3 cleavage of a gasdermin. *Nature*. 2017;547(7661):99-103.
- Yu J, Li S, Qi J, et al. Cleavage of GSDME by caspase-3 determines lobaplatin-induced pyroptosis in colon cancer cells. *Cell Death Dis*. 2019;10(3):1-20. doi:10.1038/s41419-019-1441-4
- Zhang Z, Zhang Y, Xia S, et al. Gasdermin E suppresses tumour growth by activating anti-tumour immunity. *Nature*. 2020;579(7799):415-420.
- Jiang M, Qi L, Li L, Li Y. The caspase-3/GSDME signal pathway as a switch between apoptosis and pyroptosis in cancer. *Cell Death Discov*. 2020;6(1):1-11.
- Wang Q, Wang Y, Ding J, et al. A bioorthogonal system reveals antitumour immune function of pyroptosis. *Nature*. 2020;579(7799):421-426.
- Nagarajan K, Soundarapandian K, Thorne RF, Li D, Li D. Activation of pyroptotic cell death pathways in cancer: An alternative therapeutic approach. *Transl Oncol*. 2019;12(7):925-931.
- Hanahan D, Weinberg RA. The hallmarks of cancer. *Cell*. 2000;100(1):57-70.
- Hanahan D, Weinberg RA. Hallmarks of Cancer: The Next Generation. *Cell*. 2011;144(5):646-674.
- Hanahan D. Hallmarks of Cancer: New Dimensions. *Cancer Discov*. 2022;12(1):31-46.
- He W ting, Wan H, Hu L, et al. Gasdermin D is an executor of pyroptosis and required for interleukin-1 $\beta$  secretion. *Cell Res*. 2015;25(12):1285-1298.
- Taabazuing CY, Okondo MC, Bachovchin DA. Pyroptosis and apoptosis pathways engage in bidirectional crosstalk in monocytes and macrophages. *Cell Chem Biol*. 2017;24(4):507-514.e4.
- Orning P, Weng D, Starheim K, et al. Pathogen blockade of TAK1 triggers caspase-8-dependent cleavage of gasdermin D and cell death. *Science*. 2018;362(6418):1064-1069.
- Sarhan J, Liu BC, Muendlein HI, et al. Caspase-8 induces cleavage of gasdermin D to elicit pyroptosis during *Yersinia* infection. *Proc Natl Acad Sci U S A*. 2018;115(46):E10888-E10897.
- Chen KW, Demarco B, Heilig R, et al. Extrinsic and intrinsic apoptosis activate pannexin-1 to drive NLRP3 inflammasome assembly. *EMBO J*. 2019;38(10):e101638. doi:10.15252/embj.2019101638
- Demarco B, Grayczyk JP, Bjanes E, et al. Caspase-8-dependent gasdermin D cleavage promotes antimicrobial defense but confers susceptibility to TNF-induced lethality. *Sci Adv*. 2020;6(47):eabc3465. doi:10.1126/sciadv.abc3465
- Borges JP, Sætra RS, Volchuk A, et al. Glycine inhibits NINJ1 membrane clustering to suppress plasma membrane rupture in cell death. Rothlin CV, ed. *eLife*. 2022;11:e78609. doi:10.7554/eLife.78609



30. Burden DA, Kingma PS, Froelich-Ammon SJ, et al. Topoisomerase II. etoposide interactions direct the formation of drug-induced enzyme-DNA cleavage complexes. *J Biol Chem.* 1996;271(46):29238-29244.
31. Rayamajhi M, Zhang Y, Miao E. Detection of pyroptosis by measuring released lactate dehydrogenase activity. *Methods Mol Biol Clifton NJ.* 2013;1040:85-90.
32. Gao Y, Dorn P, Liu S, et al. Cisplatin-resistant A549 non-small cell lung cancer cells can be identified by increased mitochondrial mass and are sensitive to pemetrexed treatment. *Cancer Cell Int.* 2019;19(1):317. doi:10.1186/s12935-019-1037-1
33. Pan X, Chen Y, Shen Y, Tantai J. Knockdown of TRIM65 inhibits autophagy and cisplatin resistance in A549/DDP cells by regulating miR-138-5p/ATG7. *Cell Death Dis.* 2019;10(6):1-11. doi:10.1038/s41419-019-1660-8
34. Degen M, Santos JC, Pluhackova K, et al. Structural basis of NINJ1-mediated plasma membrane rupture in cell death. *Nature.* 2023;618(7967):1065-1071.
35. Kayagaki N, Stowe IB, Alegre K, et al. Inhibiting membrane rupture with NINJ1 antibodies limits tissue injury. *Nature.* 2023;618(7967):1072-1077.
36. Cookson BT, Brennan MA. Pro-inflammatory programmed cell death. *Trends Microbiol.* 2001;9(3):113-114.
37. Xia S, Zhang Z, Magupalli VG, et al. Gasdermin D pore structure reveals preferential release of mature interleukin-1. *Nature.* 2021;593(7860):607-611.
38. Miao R, Jiang C, Chang WY, et al. Gasdermin D permeabilization of mitochondrial inner and outer membranes accelerates and enhances pyroptosis. *Immunity.* 2023;56(11):2523-2541.e8. doi:10.1016/j.immuni.2023.10.004
39. Wang J, Kang Y, Li Y, et al. Gasdermin D in different subcellular locations predicts diverse progression, immune microenvironment and prognosis in colorectal cancer. *J Inflamm Res.* 2021;14:6223-6235.

### How to cite this article

Imlilss S, Ahmadi Z, Jekki G, Eren E. Etoposide Treatment of Cancer Cell Lines Results in Nuclear Localisation of Cleaved Gasdermin D. *Eur J Biol* 2024; 83(2): 204–212. DOI:10.26650/EurJBiol.2024.1526736